Modelling of the flow with air entrainment in spillway chutes

Adriana Antunes de Melim

adrianamelim@tecnico.ulisboa.pt

Instituto Superior Técnico, Universidade de Lisboa, Portugal

Abstract:
The present study is focused on the air entrainment on conventional spillway chutes downstream of concrete dams. This numerical study has assumed as input data the discharge, the surface roughness and the channel slope, in order to determine the location of the point of inception of air entrainment, along with the main flow properties at and upstream of such location, such as the boundary layer width, the flow depth and the mean water velocity. The results were obtained through a simplified numerical model based on a semi-empirical formulation suggested in the literature on the subject. Subsequently, standard regression curves, obtained using *TableCurve* 2D® and *TableCurve* 3D®, were presented and analysed in order to estimate the main flow properties along the spillway chute in an expeditiously way. Subsequently, a study on the development of the mean air concentration along the gradually-varied flow region downstream of the inception point was carried out, in order to obtain an explicit formula for its determination. Finally, an analysis was carried out to relate the lengths of the flow region upstream of the inception point and the flow region downstream of such location, corresponding to the self-aerated gradually-varied flow.

Key-words: spillway chute, turbulent boundary layer, inception point, air-water flow, air entrainment.

1. Introduction

The construction of large hydropower plants has led to the need to develop project, construction, observation, inspection and related standards. The assessment of actual and potential risks to the downstream populations and the economic impact have determined the definition of safety measures to avoid their collapse.

Spillway chutes are safety devices of hydraulic structures that are installed in dams and whose function is to transport the inflow downstream of the dams during extreme events. In USBR (1983) it is stated that the inadequate design of the spillway represents about 23% of the dam danger. Previous studies have concluded that natural aeration of the flow serve as an effective measure in preventing cavitation damage.

Air entrainment in free surface flows has been an important subject of study in the field of hydraulic engineering, due to the bulking effect and energy dissipation (Hall, 1943, Wood, 1985, 1991, Chanson, 1996). According to various authors (e.g., Wood, 1985, 1991, Chanson, 1996 and Valero and Bung, 2016), the amount of bulking produced in the flow is a determinant and an essential aspect for the design of the height of the side walls of the spillway chute. Other relevant aspect about air-water flow, is relative to cavitation damage prevention. The air next to the floor of the spillway chute can bring two aspects: the fluid becomes compressible, making it elastic and enable to absorb the impact of pressure waves caused by the collapse of the cavitation bubbles, and reduces the effective shear stress and hence the local friction factor. This implies a greater velocity of the flow than would otherwise occur (Wood, 1991).

According to Peterka (1953) it is possible to prevent damage caused by cavitation if there is a mean air concentration in the order of 5-8%. Hence, the location of the inception point of air entrainment is essential for the design engineer in the decision to install aeration devices and their location to prevent or reduce the

damage caused by cavitation (Wilhelms and Gulliver, 2005).

The present study aims to contribute to the hydraulic design of high velocity and self-aerated flow on spillway chutes, embracing simplified numerical modelling and semi-empirical approaches.

2. Literature Review

Natural air entrainment is a phenomenon which occurs in high velocity free surface flows and can be observed in spillway chutes, as illustrated, for example, in Figure 1. Due to air entrainment, the flow becomes white and foamy (so-called “white waters”), which can be visually identified.

Figure 1 - Aviemore dam: view of the spillway chute from downstream (*https://www.facebook.com/kevin.bird.336* accessed in 02/05/2018).

Previous studies on air entrainment in free surface flows have concluded that there is a turbulent boundary layer caused by the rough spillway surface, which causes air entrainment when it intersects the free surface of the flow, defined as the inception point (Keller, Lai, and Wood, 1974). Downstream of this section, the flow is developing with increasing air entrained in depth until uniform regime flow is reached, for a long chute. From this point on, no significant changes in hydraulic or air transport are observed (Wilhelms and Gulliver, 2005).

According to various authors (e.g., Cain, 1978, Wood, 1985, 1991, Chanson, 1996, Matos, 1999), it is possible to distinguish different flow regions in spillway chutes (Figure 2).

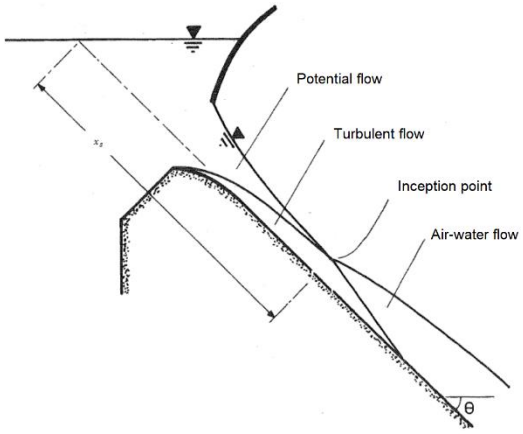

Figure 2 – Schematic representation of high velocity free surface flows (adapted from Cain, 1978).

Immediately downstream the inception point, there is a gradually varied flow region due to the air entrainment, and far downstream from point of inception the flow becomes uniform.

3. Flow properties along the chute

3.1. Inception point and flow properties

Several empirical equations have been proposed for the determination of the turbulent boundary layer development. These expressions have been based on data from laboratory experiments and flow observations in existing dams. However, until Keller and Rastogi (1977), the available relationships for the development of the boundary layer were not independent from the spillway geometry.

Keller and Rastogi (1977) proposed graphs which allow, as a function of the surface roughness and the roughness Froude number, an estimate of the location and flow depth at the inception point, by applying a k-ε turbulence model for broad range of unit discharges, channel slopes and roughness for a WES crest type. The proposed formulae were:

$$\frac{s_i}{k} = f_1(Fr_*, sen\theta) \quad (1)$$

$$\frac{h_i}{k} = f_2(Fr_*, sen\theta) \quad (2)$$

where s_i is the length from the spillway crest to the inception point section, h_i is the flow depth at the inception point, Fr_* is the roughness Froude number,

θ is the slope between the spillway chute and the horizontal plan and k is the absolute roughness.

Later, Cain and Wood (1981), relying on the proposal developed by Bauer (1951) and Halbronn (1952), where the spillway crest geometry effect is neglected, suggested the following expressions for estimating the boundary layer thickness and the velocity distribution:

$$\frac{\delta}{x_s} = a\left(\frac{x_s}{k}\right)^{-b} \quad (3)$$

$$\frac{u}{V_{máx}} = \left(\frac{y}{\delta}\right)^{1/N} \quad (4)$$

where δ is the turbulent boundary layer thickness, defined as the thickness relative to the point where the flow velocity is 99% of the potential velocity, x_s is the longitudinal coordinate from the spillway crest, y is the coordinate measured normal to the spillway chute, u is the flow velocity at y, N and b are constants, and a is a function of the chute slope.

According to Wood et al (1983) for concrete spillway chutes with low absolute roughness, N, a and b can be given by:

$$a = 0.212\ sen\theta^{-0.11} \quad (5)$$

$$b = 0{,}10 \quad (6)$$

$$N = 6 \quad (7)$$

Considering $x_s \approx s$, assumed to be a reasonable approximation if the inception point is located at a considerable distance from the spillway crest, and based on the previous equations, the following expression can be obtained (Wood, 1985, 1991):

$$\frac{\delta}{s} = 0.0212\ sen\theta^{-0.11}\ \left(\frac{s}{k_s}\right)^{-0.10} \quad (8)$$

In the present work, Eq. (8) is used, for spillway chute slopes between 5º and 75º.

3.2. Flow properties upstream of the inception point

The following main flow properties can be defined upstream the inception point:

Boundary layer displacement thickness

$$\delta_d = \int_0^{\delta}\left(1 - \frac{u}{U_p}\right)dy = \frac{\delta}{N+1} \quad (9)$$

Considering N=6 (Chanson, 1996), Eq. (9) gives δ_d = 0.14 δ.

Flow depth

According to Figure 3,

$$h = \frac{q}{V_{max}} + \frac{\delta}{N+1} \quad (10)$$

where

$$V_{max} = \sqrt{2g(N - z - hcos\theta)} \quad (11)$$

For each vertical, the flow depth is obtained iteratively.

Thickness of power loss in the boundary layer

$$\delta_e = 0.19\ \delta \quad (12)$$

Kinetic energy coefficient

Where according Chanson (1996), α can be defined as

$$\alpha = \left(\frac{V_{max}}{U}\right)^3 \frac{1}{h}\left[\left(\frac{N}{N+3}\right)\delta + (h - \delta)\right] \quad (13)$$

At the inception point α =1.058.

3.3. Flow properties downstream of the inception point

3.3.1. Definitions

Local air concentration

The local air concentration C is defined as the volume of air per unit volume and this will normally be taken as a time averaged value (Wood, 1991).

Characteristic depth for the self-aerated flow

This parameter can be defined for both model and prototype measurements as the depth where the air concentration is 90% ($y = Y_{90}$).

Mean air concentration

The mean air concentration is the depth averaged value of the air concentration, where the upper boundary is Y_{90}.

3.3.2. Uniform flow region

Mean air concentration

Initially supported by the experimental results obtained by Straub and Anderson (1958) and later supported by authors as Wood (1985) and Chanson (1993), it was verified that the uniform mean air concentration varies essentially as a function of the spillway chute slope. Several formulae have been proposed for estimating the uniform mean air concentration. Based on a reanalysis of model and prototype Matos (1999) suggested the following expression:

$$\bar{C}_u = 0.76\ sen\ \theta^{0.82} \qquad (14)$$

In the context of the present work, Eq. (14) was used.

Air concentration distribution

The air concentration distribution was determined using Wood (1985, 1991) model:

$$\varepsilon \frac{d}{dy}[\rho(1-C)] = \rho(1-C)\ V_a\ cos\theta \qquad (15)$$

where ε is the diffusivity of the average density in an air-water mixture, V_a is the fall velocity of water droplets in air and ρ the density of water.

Wood (1985) described V_a as:

$$V_a = K\ C\ y \qquad (16)$$

where $y \in [0; Y_{90}]$ and K is a constant.

Without prior knowledge of the behaviour of air concentration distribution, ε was stablished as constant and then C estimated according the following expression (Wood, 1985, 1991)

$$C = \frac{\beta'}{\beta' + e^{-\gamma' cos\theta y'^2}} \qquad (17)$$

where:

y' Normalized flow depth defined by $y' = \frac{y}{Y_{90}}$

β', γ' Parameters.

Once the free surface is defined by the local where the air concentration equals 90%, the mean air concentration can be given as (Matos, 1990, Chanson, 1993):

$$\bar{C} = \int_0^1 \frac{\beta'}{\beta' + e^{-\gamma' cos\theta y'^2}}\, dy' \qquad (18)$$

3.3.3. Gradually varied flow region

In this region, the air concentration and its distribution will vary gradually. Cain (1978), based on the experimental data gathered at Aviemore dam spillway, stated that the air concentration distribution on the gradually varied flow region will resemble that of the uniform flow region, for identical mean air concentration.

The mass of air conservation equation may be expressed as:

$$\frac{d\ q_{air}}{ds_*} = u_p - \bar{C}\ u_r cos\theta \qquad (19)$$

where $u_p$is the air velocity through the free surface, u_r the fall velocity of water droplets in air and s_* the coordinate measured from the inception point. Eq. (18) can also be expressed as (Wood, 1991, Chanson, 1993):

$$\frac{d\bar{C}}{ds_*} = \frac{u_r cos\theta}{q}\ (\bar{C}_u - \bar{C})(\ 1 - \bar{C})^2 \qquad (20)$$

In turn, Eq. (19) can be solved by an analytical integration as expressed bellow (Wood, 1991, Chanson, 1993):

$$A = K s_* + K_0 \qquad (21)$$

where A, K and K_0 can be expressed by the following equations:

$$A = \frac{1}{(1-\bar{C}_u)^2} \ln\left(\frac{1-\bar{C}}{\bar{C}_u - \bar{C}}\right) - \frac{1}{(1-\bar{C}_u)(1-\bar{C})} \qquad (22)$$

$$K = \frac{u_r cos\theta}{q} \qquad (23)$$

$$K_0 = \frac{1}{(1-\bar{C}_u)^2}\ln\left(\frac{1-\bar{C}_i}{\bar{C}_u-\bar{C}_i}\right) - \frac{1}{(1-\bar{C}_u)(1-\bar{C}_i)} \quad (24)$$

In the above equations, $\bar{C}_i$ is the mean air concentration at the inception point, taking values of 5% based on experimental results obtained at the Aviemore dam spillway. In this work, a null value was assumed for this parameter, except for the comparative analysis of results obtained by Cain (1978) and by the numerical model.

4. Numerical model implementation: simplified hypotheses

In this study, the methodology to determine the characteristics of the flow upstream of and at the inception point was based on the following hypotheses:

- The spillway chute has a rectangular cross-section.
- Simplified inlet chute flow conditions, as per Figure 3.
- Negligible head loss between the reservoir and the spillway chute.
- The pressure distribution along the chute is hydrostatic.
- Water and air behave as non-miscible fluids.
- The air-water flow is homogeneous, and the air velocity is equal to the water velocity in the flow direction.
- The equations of conservation of mass, momentum and energy are applicable to each elementary volume of the fluid, considered homogeneous, being necessary to know the concentration of air at any point in the fluid.
- The rate of air entrainment is constant.
- Variations in velocity from the inception point to the uniform regime are negligible.

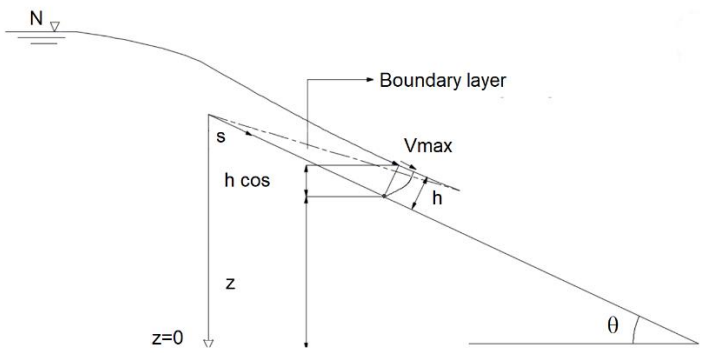

Figure 3- Schematic representation for the calculation of the flow depth upstream of the inception point.

5. Results

5.1. Flow properties upstream of the inception point

After applying the numerical procedure described previously, 273 different practical combinations of q, K and θ we analysed, as showed in Table 1.

Table 1 – Input data for the numerical model.

Variable	Input data
q (m^2s^{-1})	1; 5; 10; 15; 20; 30; 40; 50; 60; 70; 80; 90; 100
K $(m^{1/3}s^{-1})$	50; 75; 90
θ (°)	10; 20; 30; 40; 50; 60; 70

The analysis of the results obtained in this study for the flow upstream of the inception point indicates that the spillway slope has a significant impact on the normalized flow depth along the chute, as showed in Figure 4.

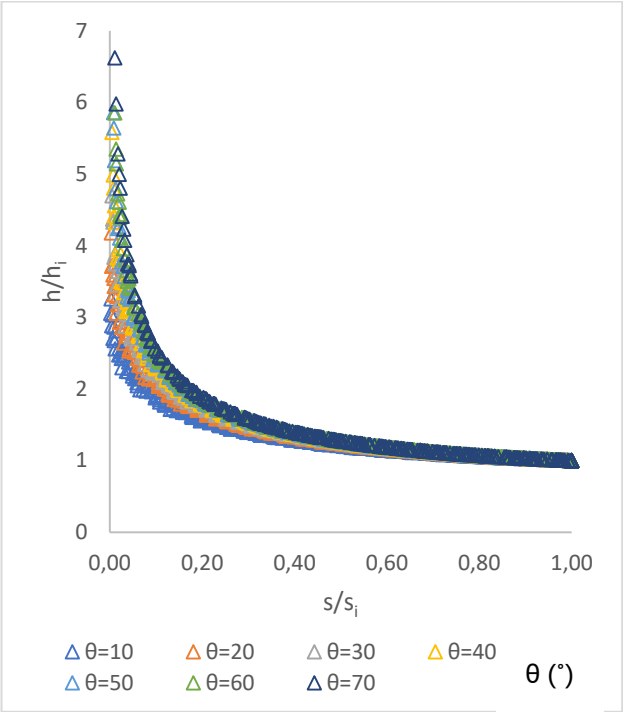

Figure 4 - Results obtained by the numerical method for unit discharges of 5, 20, 40, 100 m^2s^{-1}, spillway slopes of 10˚, 20˚,30˚; 40˚; 50˚, 60˚, 70˚ and Manning-Strickler coefficients of 50, 75, and 90 $m^{1/3}s^{-1}$.

Also, the results show that the influence of the slope is attenuated for $s/s_i>0,5$. In other terms, the impact of θ becomes practically negligible in half of the non-aerated flow reach. Regression curves were then analysed using the *TableCurve* 2D® software.

For all the tested unit discharges, slopes and Manning-Strickler coefficients, the following equation was obtained

$$\frac{h}{h_i} = \frac{1}{a + b\sqrt{\frac{s}{s_i}}} \qquad (25)$$

where a and b are expressed as function of the chute slope:

$$a = \frac{1}{2{,}428 + 6{,}434\ tg\theta} \qquad (26)$$

$$b = \frac{1}{0{,}835 + \frac{0{,}209}{\sqrt{tg\theta}}} \qquad (27)$$

Subsequently, these regression curves were validated for different combinations of unit discharges, spillway slopes and Manning-Strickler coefficients.

Figures 5, 6 and 7 show the comparison and validation of the regression curves with the numerical data for θ=10˚, 40 and 70˚.

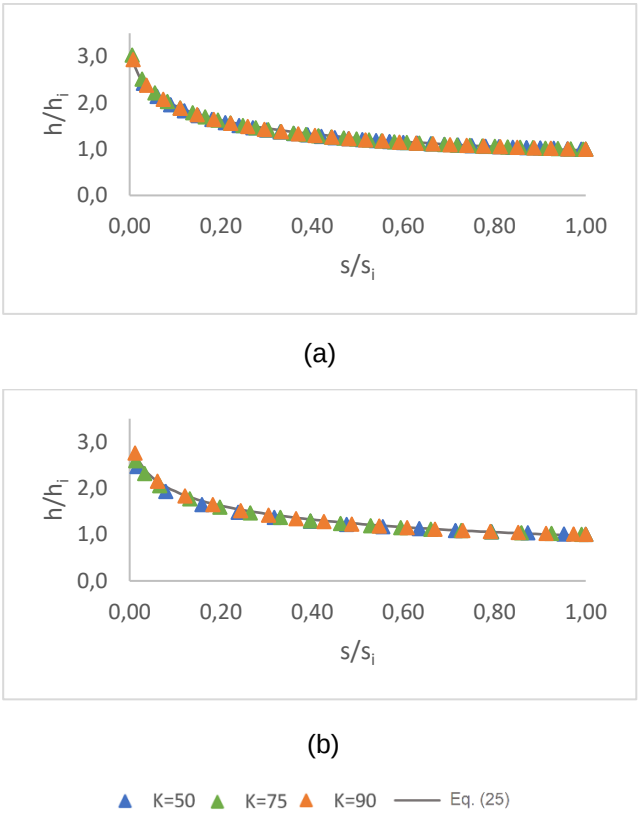

Figure 5 - Normalized flow depths along the chute for θ=10˚: (a) q=5 m^2s^{-1}; (b) q=20 m^2s^{-1}.

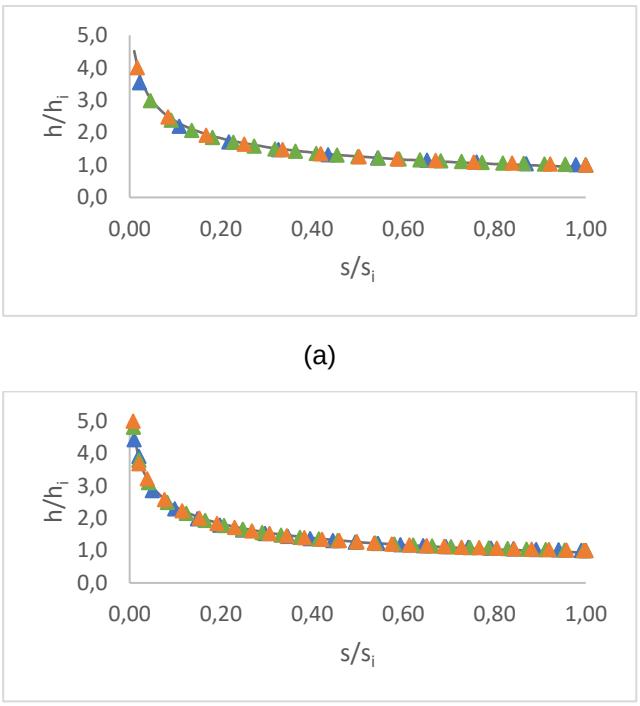

Figure 6 - Normalized flow depths along the chute for θ=40˚: (a) q=5 m^2s^{-1}; (b) q=20 m^2s^{-1}.

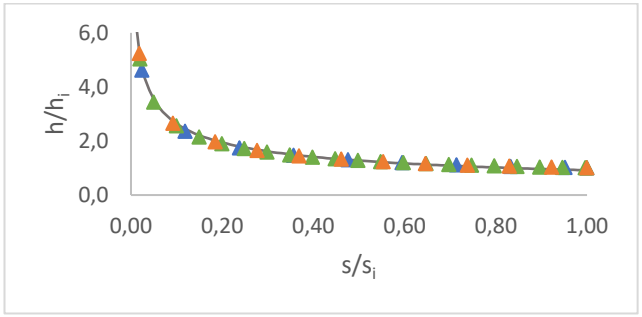

(a)

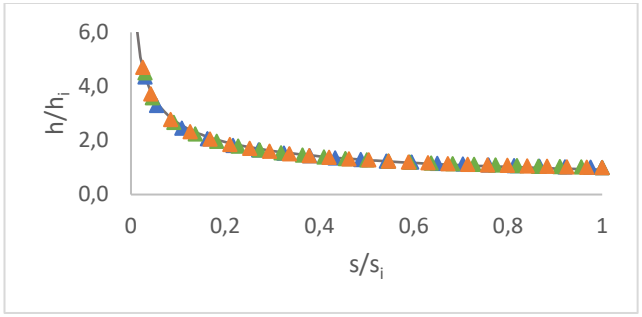

(b)

Figure 7 - Normalized flow depths along the chute for θ=70˚: (a) q=5 m^2s^{-1}; (b) q=20 m^2s^{-1}.

In general, an excellent agreement was obtained between the regression curves and the numerical model.

5.2. Flow properties downstream of the inception point

5.2.1. Development of empirical formulae

The subsequent study of the mean air concentration along the spillway chute downstream of the inception point was based on the analytical integration of Eq. (21) to (24). Figure 8 shows the results obtained for the 30˚ spillway chute.

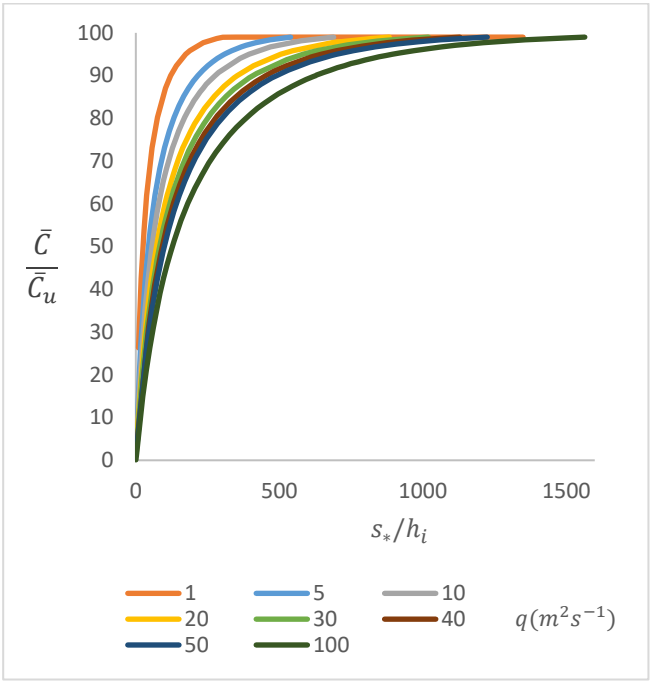

Figure 8 – Mean air concentration along the spillway chute: results obtained from Eq. (21) to (24), for a slope of 30˚ and a range of flow rates.

Similar to the previous study, it was intended to analyse a practical and simple regression surface which could give the mean air concentration along the gradually flow regime as

$$\frac{\bar{C}}{\bar{C}_u} = \Phi\left(sen\theta; \frac{h_c}{k}; \frac{s_*}{h_i}\right) \quad (28)$$

According to Eq. (28) and by using the *TableCurve* 2D® software, the following expression was obtained:

$$\frac{\bar{C}}{\bar{C}_u} = \frac{a\,\frac{s_*}{h_i}}{b + \frac{s_*}{h_i}} \quad (29)$$

where a and b are given as:

$$a = 132.33 - 31.33\sqrt{sen\theta} \quad (30)$$

$$b = -82.85 + \frac{(-16.2)}{ln(sen\theta)} + 3.25\sqrt{\frac{h_c}{k}} \quad (31)$$

Figures 9 and 10 show the results obtained by solving the analytical integration of Eq. (21) to (24) and from Eq. (29) to (31), for 10, 40 and 70˚ chute slopes and for unit discharges of 5 and 20 m^2s^{-1}, respectively.

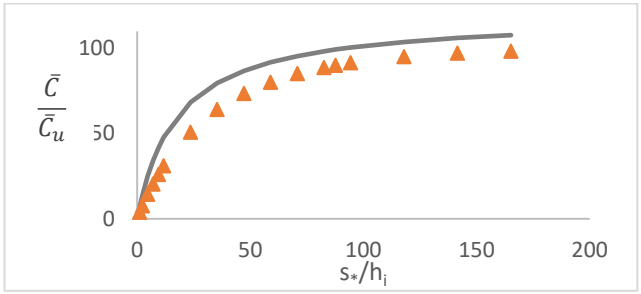

(a)

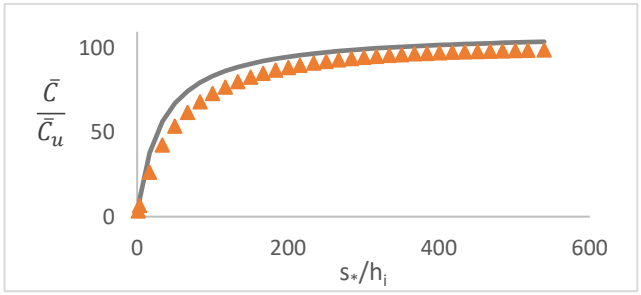

(b)

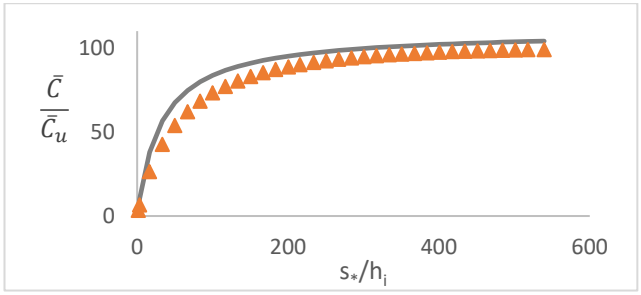

(c)

Figure 9 - Mean air concentration along the spillway chute: results obtained from Eq. (21) to (24) and from Eq.(29) to (31), for q = 5 m^2s^{-1} and slope equal to: (a) 10˚; (b) 40˚ and (c) 70˚.

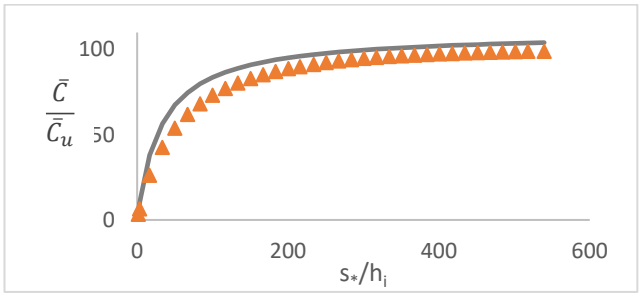

(a)

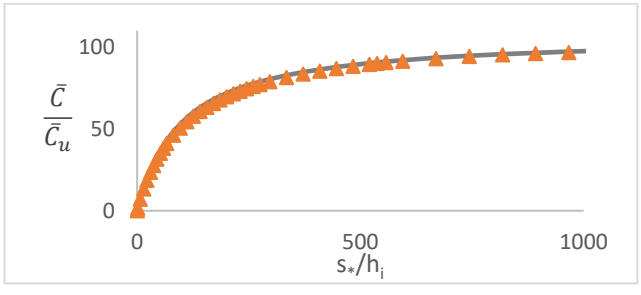

(b)

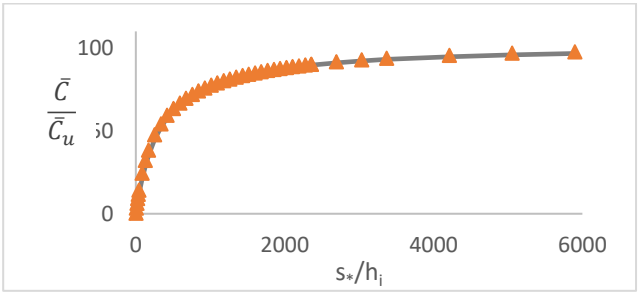

(c)

Figure 10 - Mean air concentration along the spillway chute: results obtained from Eq. (21) to (24) and from Eq.(29) to (31), for q = 20 m^2s^{-1} and slope equal to: (a) 10˚; (b) 40˚ and (c) 70˚.

5.2.2. Method validation

In order to validate the results obtained from Eq. (29) to (31), these were compared with the experimental data from Cain (1978), for q (m^2s^{-1}), θ (˚) and k_s (m) as described in Table 2.

Table 2 – Prototype data from Cain (1978).

q (m^2s^{-1})	2.23	3.15
θ (˚)	45	
sen(θ)	0.707	
u_r (m/s)	0.4	
k_s (m)	0.001	

In Table 3, the location and flow depth at the inception point from Cain (1978) are presented.

Table 3 – Flow depth, location and characteristic velocity at the inception point, from Cain (1978).

q (m^2s^{-1})	2.23	3.15
h_i (m)	0.152	0.194
s_i (m)	18.4	23.8
V_{90} (ms^{-1})	16.0	18.2

Figures 11 and 12 show the mean air concentration along the chute obtained from the previously described methods versus Cain's (1978) experimental data.

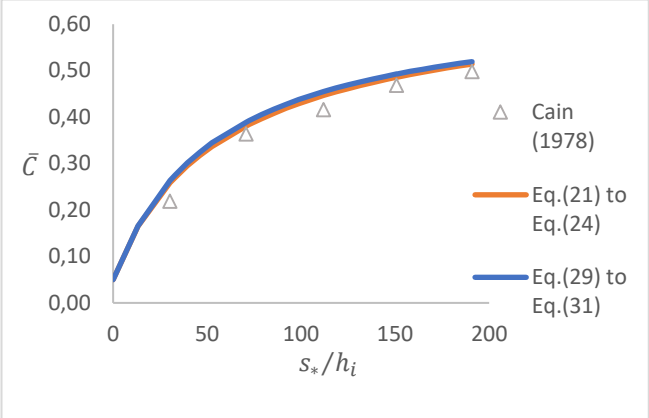

Figure 11 – Mean air concentration as function of distance to the inception point for q = 2.23 m^2s^{-1}.

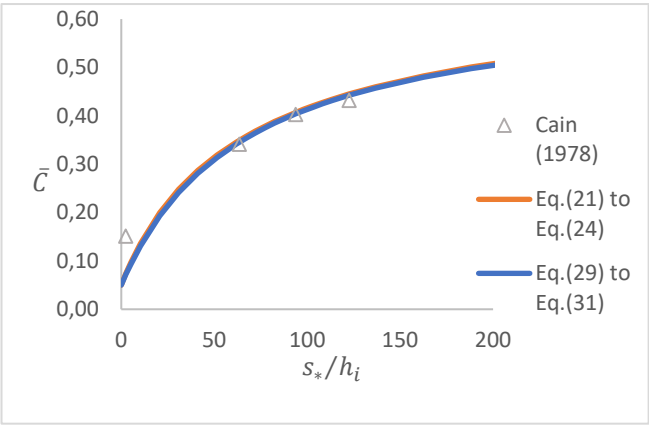

Figure 12- Mean air concentration as function of the distance to the inception point for q = 3.15 m^2s^{-1}.

Length of the gradually-varied, self aerated flow region

Using the software Table Curve 3D® and as input data the results obtained for the length of the flow region upstream of the inception point (s_i) and the flow region of the self-aerated gradually-varied flow (s_{u*}), the following relation was obtained:

$$\frac{s_{u*}}{s_i} = e^{a+bsen\theta^3+c\ ln\left(\frac{h_c}{k}\right)} \qquad (32)$$

The parameters a, b and c depend on the criterion used to define the uniform regime, as described in Melim (2018).

As an example, Figure 13 shows the regression surface of the results obtained when the mean air concentration attains 90% of that relative to the uniform flow regime.

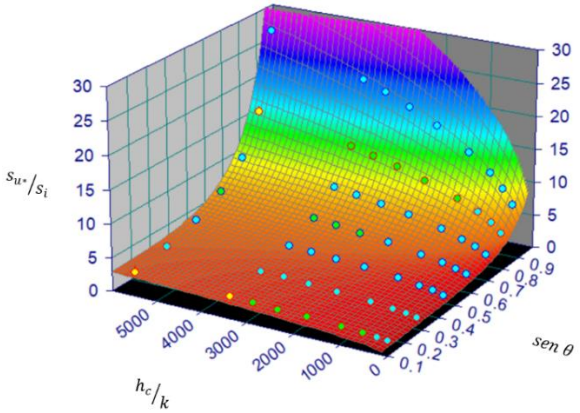

Figure 13 – Normalized distance to attain uniform flow: regression surface of the results obtained when the mean air concentration attains 90% of the uniform mean air concentration.

6. Conclusions

The main purpose of the present study was to provide a contribution to the estimation of relevant flow properties of high velocity flow with self-aeration in conventional spillway chutes.

The following conclusions can be drawn from this study:

- A simple formula can be applied to estimate the normalized flow depth along the chute, as a function of a normalized distance from the crest and the chute slope.
- A formula can also be used to estimate the mean air concentration along the chute, as a function of a normalized distance from inception, the chute slope, and the uniform mean air concentration. The fit was found to be quite good, but for flat slopes and small unit discharges.
- The distance for uniform flow to be attained can also be estimated from a dimensionless formula developed in this study.

Acknowledgements

The author thankfully acknowledges Professor Jorge Matos (IST) for all the supervision and support of the M.Sc. thesis.

References

Bauer, W. (1951). The development of the turbulent boundary layer on steep slopes. University of Iowa, USA.

Cain, P. (1978). Measurements within self-aerated flow on a large spillway, Ph.D. thesis, Ref. 78-18, Department of Civil Engineering, University of Canterbury, Christchurch, New Zealand.

Cain, P., Wood, I. (1981). Measurements of self-aerated flow on a spillway. *Journal of Hy*draulic Engineering, 107, 1407-1242.

Chanson, H. (1993). Self-aerated flows on chutes and spillways. *Journal of Hy*draulic Engineering, 119(2), 220-243.

Chanson, H. (1996). Air bubble entrainment in free-surfa*ce* turbulent shear flows. Academic Press, London.

Halbronn, G. (1952). Etude de la mise en régime des écoulements sur les ouvrages à forte pente. *La Houille Blanche (3)*, 347-371 (in French).

Hall, L. (1943). Entrainment of air in flowing water, A symposium: Open channel flow at high velocities. *Trans. (ASCE)*, 1943.

Keller, R. J., Lai, K. K., Wood, I. R. (1974). Developing region in self aerating flows. *J. Hyd. Div., 100*(HY4), 553-568.

Keller, R. J., Rastogi, A. (1975). Prediction of flow development on spillways. *J. Hyd. Div., 101*(HY9), 553-568.

Keller, R. J., Rastogi, A. (1977). Design chart for predicting critical point on spillways *J. Hyd. Div., 103*(HY12), 1417-1429.

Melim, A. (2018). Modelação do escoamento com emulsionamento de ar em descarregadores de cheias em canal. M.Sc. thesis, IST, Lisbon, Portugal (in Portuguese).

Matos, J. (1990). O Arejamento como medida de protecção contra a erosão de cavitação em obras hidráulicas. M.Sc. thesis, IST, Lisbon, Portugal (in Portuguese).

Matos, J. (1999). Emulsionamento de ar e dissipação de energia do escoamento em Descarregadores em Degraus. Ph.D. thesis, IST, Lisbon, Portugal (in Portuguese).

Peterka, A. J. (1953). The effect of entrained air on cavitation pitting. 5th IAHR Congress, Joint meetin*g paper, IAHR/ASCE*, 507-518.

Straub, L., Anderson, A. (1958). Experiments on self-aerated flow in open channels. *J. Hydraul. Div., 84*(7), 1-35.

USBR (1983). Safety of existing dams: Evaluation and improvement.Water Resources Technical Publication. U.S. Department of the Interior, Denver.

Valero, D., Bung, D. B. (2016). Development of the interfacial air layer in the non-aerated region of high-velocity spillway flows. Instabilities growth, entrapped air and influence on the self-aeration onset. *International Journal of Multiphase Flow*, 66-74.

Wilhelms, S., Gulliver, J. (2005). Bubbles and waves description of self-aerated spillway flow. *J. of Hydraulic Research, 43, No. 5*, 522-531.

Wood, I.R. (1983). Uniform region of self-aerated flow, *Journal of Hydraulic Engineering*, ASCE, Vol.109, No. 3, pp. 447-461.

Wood, I.R. (1985). Air-water flows, Preprints of the 21st IAHR Congress, Melbourne, Australia, Keynote Address, pp. 18-29.

Wood, I.R. (1991). Free surface air entrainment on spillways, in Wood, I.R. “Air entrainment in free-surface flows”, IAHR, Hydraulic Structures Design Manual 4, Hydraulic Design Considerations, A. A. Balkema, Rotterdam, the Netherlands, 55–84.